Real-Time Road Pothole Mapping Based on Vibration Analysis in Smart City

Dong Chen, *Member, IEEE*, Nengcheng Chen, Xiang Zhang, and Yuhang Guan

***Abstract*—Vehicle-road collaboration is inseparable for smart cities, and the potholes detection is an essential direction in vehicle-road collaboration. With the development of surveying and mapping technologies, road potholes detection accuracy has improved in recent years. However, the legacy detection methods do not have the ease of service and real-time observation capability, and thus, the potholes in the road cannot be mapped in time. To solve this key issue, we proposed a reflectometry method to realize real-time potholes observation with vibration signals analysis and Spatio-temporal trajectory fusion. We further developed several prototype devices for validation. These prototype devices measure the acceleration signal mounted on the wheel steering lever and implement edge signal processing and Spatio-temporal information fusion on the prototype. Observation results and Spatio-temporal information are been rapidly transmitted to the sensing server via narrow band Internet of Things. Results and analyses demonstrated that this method successfully enabled the potholes observation in real-time through light and a rapidly deployable platform that relies on repeated trajectory data from the vehicle. Results also demonstrated that this method was not limited by vehicle type, speed, or engine operating condition. In the road experiment, the proposed method provided stable, efficient, and real-time potholes observation results. Compared with traditional methods, the method reduces costs and improves sensing efficiency based on Spatio-temporal trajectory fusion, and potholes information can be prompted in real-time. This innovation provides a strategic exploration and thinking to deal with road potholes in real-time sensing.**

***Index Terms*—Automated instruments, road surface observation, signal processing, smart city, Spatio-temporal fusion, vibration processing.**

NOMENCLATURE

DSM	Digital surface model.
FFT	Fast Fourier transform.
GNSS	Global Navigation Satellite System.
GIS	Geographic Information System.
IoT	Internet of Things.
LiDAR	Light detection and ranging.
NVH	Noise, vibration, harshness.
NB-IoT	Narrow band Internet of Things.
OBD	On-board diagnostics.
RMS	Root mean square.
RPM	Revolutions per minute.
SAR	Synthetic aperture radar.

Manuscript received 7 June 2022; revised 3 August 2022; accepted 16 August 2022. Date of publication 19 August 2022; date of current version 2 September 2022. This work was supported by the National Key Research and Development Program of China under Grant 2018YFB2100500. *(Corresponding authors: Nengcheng Chen; Xiang Zhang.)*

Dong Chen is with the State Key Laboratory of Information Engineering in Surveying, Mapping and Remote Sensing, Wuhan University, Wuhan 430079, China (e-mail: dong_chen@whu.edu.cn).

Nengcheng Chen and Xiang Zhang are with the National Engineering Research Center of Geographic Information System, School of Geography and Information Engineering, China University of Geosciences, Wuhan 430074, China, and also with the Hubei Luojia Laboratory, Wuhan 430079, China (e-mail: chennengcheng@cug.edu.cn; zhangxiang76@cug.edu.cn).

Yuhang Guan is with the National Engineering Research Center of Geographic Information System, School of Geography and Information Engineering, China University of Geosciences, Wuhan 430074, China (e-mail: 1105110750@qq.com).

Digital Object Identifier 10.1109/JSTARS.2022.3200147

I. INTRODUCTION

ROADS are the arteries and veins of a modern economy as critical infrastructure in our cities [1], [2]. The real-time observation and analysis of road surface information are vital for drivers, highway management, and future automatic driving in smart cities [3]. High-quality road condition is the foundation of urban development. However, there will be numerous imperceptible roughness after years of usage. These potholes will stimulate the vehicle structure noise and affect the vehicle's NVH, resulting in a bad experience for drivers and passengers [4]. Once a pothole is visually observable and unnoticed or unavoidable by the driver, it is likely to damage the vehicle's suspension, move out of the driving lane, or cause a rear-end collision by emergency braking, thus threatening the life and health of the driver and passengers.

There is a strong willingness from the government and road management to locate and repair roads promptly, but it is still a great challenge to timely and accurately map these potholes on roads. At present, the widely used method is manual inspection. Although this method can ensure accuracy, it requires a huge amount of labor and time. With the development of smart cities, numerous cities provide a "smart city management platform" [5], [6], [7] to improve the richness of sensory data through "crowdsourcing" images and GNSS positioning from citizens [8], but this method is still inefficient for real-time road observation. To meet this challenge, it is necessary to propose an efficient and real-time observation system to discover the road surface potholes. For this purpose, several methods can be used to observe damaged road sections rapidly, including laser scanning methods [9], [10] [three-dimensional (3-D) laser scanning], machine vision (stereo machine vision) [12], [13], [14], airborne Synthetic Aperture Radar [15], Ground Penetrating Radar [16], and vibration [17].

First, the laser scanning method is a noncontact active measurement system that allows 3-D data acquisition over large,

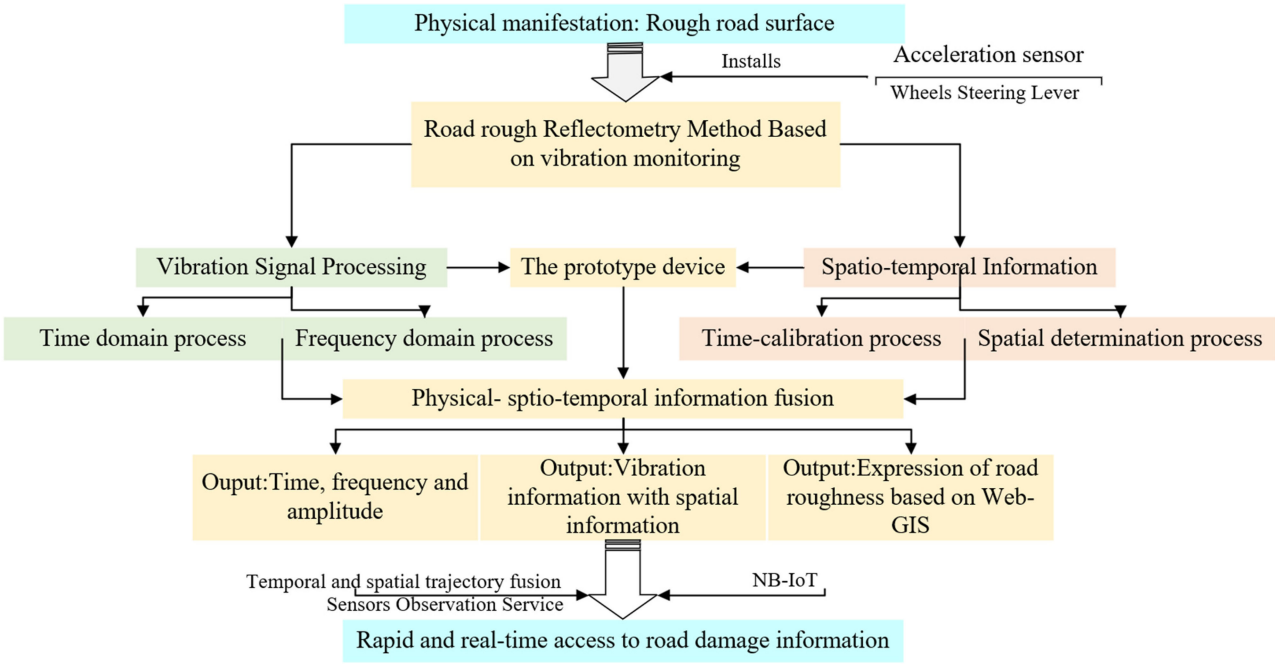

Fig. 1. Methodology architecture of road quality assessment based on vibration with real-time GIS. The method consists of vibration signal processing and the fusion of Spatio-temporal information. The anomaly of the road is observed by the time-frequency analysis method. The anomaly occurrence signals are recorded by the time stamp via the prototype device and matched with the Spatio-temporal information. Finally, the road damage observation result is loaded by Spatio-temporal information.

high-density spaces. Laser scanning is featured by high accuracy of measurement points. By road scanning, data filtering, and point cloud processing can generate the digital surface model to discover the potholes. Although the laser scanning method can generate a high-precision road model for road damage identification, the laser scanner needs to be mounted on a specific vehicle. It possesses high cost and high computing requirements and thus is not conducive to real-time observation.

Second, machine vision analysis of road potholes includes two strategies. One is a single-camera recognition, where a vision sensor on the front windshield photographs the road surface to monitor potholes in real-time while driving. For example, the Korea Institute of Civil Engineering and Construction Technology executed this research in 2016. The second way uses multidirectional camera recognition and modeling. For example, Tesla has been working on vehicles equipped with automatic driving hardware for real-time processing since 2020. The machine vision can be more easily deployed in some civilian cars while providing a method with high real-time performance. However, this system requires vast computing power and cannot be used in all vehicles. Additionally, cameras to record road information may run afoul of privacy breach, illegal surveying.

Third, the vibration assessment is a classical method, and Dodds and Robson [18] proposed "The description of road surface roughness" and laid the theoretical foundation of vibration assessment. According to this method, researchers and engineers believe that the structural vibration of a vehicle is influenced by the road surface condition, which affects the vehicle's NVH performance. Therefore, researchers analyze and evaluate the vibration data while driving the car or use a vehicle bump accumulator. However, portability is an issue to consider when using this assessment method. Wu et al. [19] proposed a smartphone with triaxial accelerometer for vibration signals acquisition to improve its usability. We believe there are a lot of potential improvements in this approach. For example, it is easy to find the vibration observation of the smartphone is relative to the entire vehicle structure rather than the structure that is most sensitive to the road surface. Meanwhile, the electromagnetic characteristics of the smartphone and the user interaction from message notifications and incoming calls will certainly have negative impacts on continuous observation.

To address this issue, this context provides a real-time method for rapidly identifying road potholes. Furthermore, we developed prototype equipment for experiments. The prototype uploads the observation results of roughness and the Spatio-temporal trajectory information [20] to the city service center via IoT. Based on the Web-GIS service, a map of urban potholes with the high spatial and temporal resolution is easily generated. We believe this proposed method enhances the real-time perception of road conditions in smart cities.

II. Method

In this context, we propose a vibration-based method for potholes mapping with real-time GIS. This method is consisted by vibration acquisition, data processing, and Spatio-temporal fusion of roughness information, as shown in Fig. 1.

A. Vibration Signal Acquisition

The acquisition of vibration is the observation source of the research, and the selection of the correct measurement method

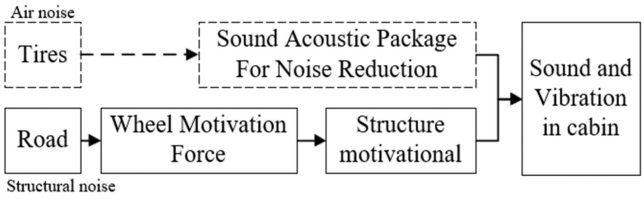

Fig. 2. Transmission process of noise in vehicles.

can improve the reliability of vibration-based observations. For vehicles, the car's road noise can be divided into air noise and structure noise, as shown in Fig. 2

Structural noise refers to the excitation of tires by the roughness of the road surface when the vehicle is driving. Thus, the noise is transmitted from the chassis and body structure to the interior of the vehicle. For the measurement of structural noise, the selection of the accelerometer measurement point and the selection of the acceleration direction are critical. Kindt et al. [21] proposed that the structural road noise is formed by the constant local compression and release of the tire-road contact to produce vertical force and the constant rolling and squeezing of the tire-road contact to produce longitudinal force. The excitation force is transmitted through the tire and rim coupling to the axle. Moreover, the axle is transmitted to the chassis and body to form the noise. The noise and vibration frequency are generally at 20–400 Hz. Furthermore, Zhao et al. [22] concluded the general 80 Hz for the effect of the uneven road surface. This context conducted a series of experiments to address this issue in the experimental section [22].

Air noise is the frictional sound generated by the tires and the road surface, which is transmitted through the air to the interior of the vehicle and can be acquired by sound pick-up equipment. The frequency range of air noise is usually higher than 600 Hz. Not only will the quality of the road surface affect the air noise of the vehicle, but the type of tire, grain, tire pressure, and other parameters will affect the measured value of air noise. For the cockpit, the driver and passenger conversations, engine noise, car audio, or active noise canceling systems will bring uncertainty to this approach. Although both the vibration frequency range and the measurement method, the reflectometry of pavement roughness based on structural noise and vibration are more appropriate for the study of this context.

In addition to the measurement method, the context requires selecting a more reliable position to install the acceleration sensor to provide a trustworthy reflectometry accuracy of the pavement roughness. It can be seen that the wheel steering lever is the primary module in the vehicle to contact the vibration generated by the excitation source. At the same time, the Steer-by-Wire technology used by some vehicles will significantly reduce the "road sense" by abolishing the mechanical connection between the steering wheel and the wheels [23]. Therefore, it is reasonable and informative to directly install acceleration sensors on the steering control mechanism in the vehicle. The axial direction of the acceleration sensor will be analyzed and verified experimentally in this context. Therefore, triaxial (vertical, front-back horizontal, and left-right horizontal) accelerometers will be applied in the experiment section.

B. Data Processing

This article proposes the following signal analysis and processing method in the time and frequency domains. These algorithms develop and implement by National Instrument LabVIEW and embedded in a computer integrated with the aforementioned data acquisition modules. The vibration signal processing is divided into two parts: The program identifies prominent pavement damage areas that may generate strong impact signals at first. Second, it identifies rough road areas through the fusion analysis method of time domain and frequency domain signals.

1) Preliminary Processing: First, a signal processing method needs to evaluate the vibration intensity and stability. It determines if there are significant defects on the pavement. This method is usually processed by calculating the average value of the vibration signal (averaging) and calculating the "quadratic mean " (root-mean-square, rms) [24]. Rms measurements usually acquire the fast change dynamic signals to represent energy. Considering that, the tires of a car driving on the road will be selected to for rms measurement. These road defects can be captured directly by a single time-domain signal processing method. The rms level of a continuous signal S(t) from time t0 to time t1 is given by the

$$S_{\text{rms}} = \sqrt{\frac{1}{(t1 - t0)} * \int_{t0}^{t1} S^2(t)\, dt} \tag{1}$$

where:

t1: Ending Time of Acquisition;
t0: Starting Time of Acquisition.

Although it is impossible to obtain reliable results, because the average value cannot emphasize the alluvial signal power, The quadratic mean (rms) can help the system achieve remarkable results through the alluvial signal power. In other words, it can easily determine the road quality information from the surface. Since this approach is in the primary stage of the system, it is always in operation to achieve dynamic observation of the entire process, which is critical for real-time rms calculations. Thus, in this context, the signal processing methods are proposed to achieve fast reflectometry of road conditions with moderate damage [25].

2) Vibration Analysis Based on Time-Frequency Fusion: This context proposes a real-time fusion method based on rms and wavelet analysis of vibration signals to reflect and analyze road damage in moderation.

There are two essential parts to this process. First, the real-time rms determines whether there are any anomalies within the observed time window. The importance of this method is that different road conditions or vehicle conditions affect the vibration signal of the road with moderate damage, and real-time rms calculations can judge the overall condition of the road at successive times. The real-time rms calculation evaluates the similarity of two adjacent time-sampled signals during driving. If two consecutive adjacent signals possess a low degree of similarity, it basically indicates that the overall road condition has changed. The real-time rms calculation plays a role in this method to calibrate the sensing system in real-time. Real-time

correlation analysis will set a high similarity coefficient as standard vibration data in the ensuing calculation. These data will act as a low cutoff filtered signal used for the data collected during system operation, which will minimize the effect of signal noise on the extraction of eigenvalues from the observation system. However, the existence of overall road condition change will also influence the rms similarity, resulting from low reliability. This requires the following frequency analysis.

The FFT does enable time vs. amplitude (time-domain signal) to frequency versus amplitude (frequency-domain signal). Nonetheless, the vibration signals are nonperiodic and nonstationary in reality, FFT cannot provide high-resolution results when analyzing the transient signals. Because the FFT system should define the shape and length of the analysis window at first, and the time and frequency resolution in its signal analysis fix according to the window. At the same time, the FFT may cause the signal to be mixed in the analysis of random vibration signals with wide frequency bands. This issue brings misjudgment to the prototype system. Therefore, we kept the FFT method in developer mode to perform manual signal analysis in the prototype system for the experiment used. However, in automatic acquisition and processing, it will not be possible to empower automation due to the drawbacks mentioned above of FFT. The wavelet analysis in vibration signal analysis is characterized by localization and variable resolution (i.e., integration of time, amplitude, and frequency) in the time and frequency domains. Also, wavelet analysis has multiresolution time-frequency localization and fast linear multichannel bandpass filtering. These features are well suited for the rapid assessment of road quality based on vibration interfaces. Equation (2a) is the definition of wavelet transform (analytical wavelet). And (2b) is the specific form of the wavelet transform, the primary function is not a sinusoidal function, and the parameters α and β can be changed in the wavelet transform process. It can be fast deteriorating on both terminal sides in the time domain, and its frequency-domain band works as the bandpass filtering of vibration signals. Changing the parameter α changes the bandwidth and center frequency position of bandpass filtering. These properties constitute the frequency localization of the wavelet method

$$W_f\ (\alpha,\beta)\ = |\alpha|^{-\frac{1}{2}}\ \int_{-\infty}^{\infty} f\,(t)\,\overline{\psi\left(\frac{t-b}{a}\right)}\,dt \tag{2a}$$

$$\psi_{a,b}\ (t)\ = |a|^{-\frac{1}{2}}\ \psi\left(\frac{t-b}{a}\right)\ a,b\in\ R,\ a\neq 0. \tag{2b}$$

In the time-frequency analysis of vibration signal, the continuous rms calculations allow identifying information about roads with big potholes. Then, the fusion of rms and wavelet analysis allows the identification of the road qualities of the most irregular. These continuous signals are separated into an interval of one second during the processing, which matches the time stamp of the device. At the same time, the maximum value index is established in the program to obtain the amplitude peak signal in each set of the spectrum (i.e., a processing interval) with its corresponding occurrence time and frequency. Eventually, the time and frequency information corresponding to the maximum magnitude of each set of spectrum data will be saved in the database.

C. Fusion of Spatial-Temporal Information

The method in Section II-B only acquires the impact signal of irregular road surfaces, which does not reflect the real-time road potholes in smart cities. To establish this capability, the vehicle's continuous positioning data (i.e., trajectory data) must be acquired, i.e., the GNSS data. By recording the time and position information from the GNSS module in the database, the Spatio-temporal trajectory can be provided for the moving object (vehicle). Fig. 3 shows the method of matching anomalous vibration information of road surface with Spatio-temporal information.

In this context, a prototype builds in a micro-x86 environment, and the method uses GNSS to obtain positioning information. At the same time, this method combines the characteristics of fast observation of road conditions by vehicle vibration information, which is necessary for mapping road potholes based on Spatio-temporal trajectories. When the system is in real-time acquisition, the system continuously receives the GNSS data message according to the national marine electronics association (NMEA) protocols. It parses the coordinates and timing information in the messages in real-time and stores them in the database with time-stamped attributes in the device. Latitude and longitude record spatial information accurately, but the vast amount of data will lead to inefficient retrieval and matching in the background. Therefore, a data splitting method named Google Plus Codes describes the spatial location efficiently. Google Plus Code belongs to a gridding method for describing geospatial locations. This method is based on the geospatial dissection, which divides geospace into arbitrary grids with multiscale and assigns globally unique codes as string-type [26], [27]. Thus, it realizes the multiscale area location identification and geospatial correlation at different scales. Using grid codes can improve the query efficiency of spatial databases and web services through a service model based on location reception and information matching at the edge. In fact, besides Google Plus Code, there are other definition methods such as Beidou Grid Code. In the database, a string field replaces two floating-point fields in the database, such as 8P2PFJG4+XC, representing LAT: 30.477438N, LON: 114.606063. Through analysis of vibration signals, the program outputs the maximum magnitude and frequency data with time attributes. Finally, these data will be mapped with spatial location data in the database. This approach enables the Spatio-temporal trajectory data to carry information about the intensity of road vibration.

In order to obtain reliable and valid data, a single observation is not universal and opportunistic. Therefore, the observation data uploaded to the cloud server (space-time information platform) and the spatial information of the road (Plus codes ID in the database) with an abnormal vibration signal for the first time will be marked and alarmed. When the abnormal vibration signal appears several times at the same plus codes will be judged as an irregular road surface. This mechanism will improve the credibility of the observation results.

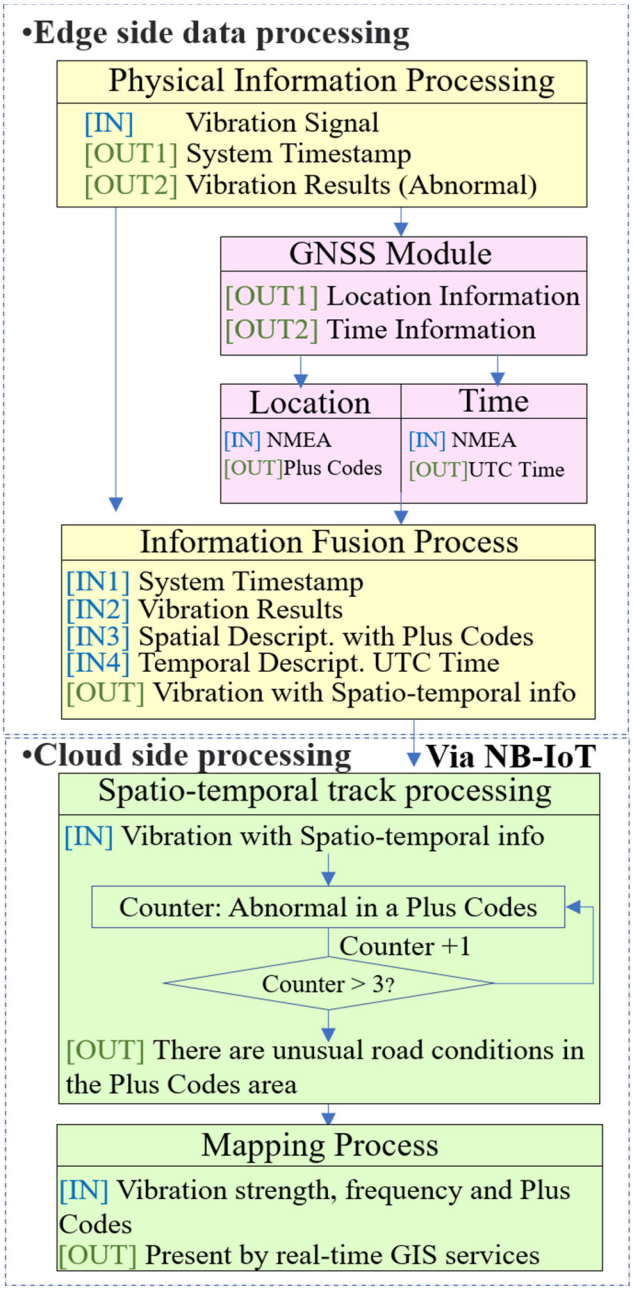

Fig. 3. Method of precise matching of Spatio-temporal information. It consists of the edge side and the Cloud side. The edge side consists of sensors, signal processing, and network modules; the cloud provides real-time GIS services to present the results. The edge side installed on the vehicle for acquiring and analyzing the vibration signals and the abnormal signals and the occurrence timestamp is recorded in the database. Meanwhile, the NMEA messages obtained by the GNSS module will be parsed into spatial information (expressed in Plus Codes) and temporal information (expressed in UTC time). These anomalies observation of road surface is fused at the edge side and sent to Cloud by the NB-IoT. The Cloud side provides real-time information service with road anomaly information by the occurrences of Plus Codes that contain anomalous observations of the road surface.

III. Experiment and Results

A vibration-based road quality reflectometry system is proposed to verify the validity and generalizability. The experimental equipment includes hardware with real-time vibration signal analysis and acquisition with NB-IoT capability. The experimental vehicles include saloon cars and sport utility vehicle (SUVs). They tested on a closed test site (with a high-quality road surface and high-speed driving for testing) and daily road scenarios in the Guanggu East area in Wuhan, China.

TABLE I
Closed-Course Experiment Test Parameters

Group	Distance (m)	Speed range (km/h)	Stable speed (cruising) (km/h)
A	1500	30–120	80
B	1800	120–190	140

A. Experimental Device Setup

The experimental prototype device used in this article consists of an edge computing device with x86 architecture executing the algorithms and data acquisition programs, a National Instrument 9234 data acquisition interface card, and a Bruel&Kjaer 4535-B three-axis acceleration sensor. The device integrated with GNSS and NB-IoT modules to fuse the vibration information and spatial-temporal parameters in real-time. Fig. 4 presents the core hardware and software in the experiment protocol devices.

The acceleration sensor used to collect vibration signals is mounted on the steering lever of the vehicle, with the X, Y, and Z directions of the sensor indicated as perpendicular, parallel, and horizontal to the steering lever, respectively. It helps to analyze the vibration in three different directions when the steering wheel drive lever brings about road defects to identify the most significant acceleration direction. Figs. 4(a) and 5 present the mounting position of the triaxial accelerometer.

B. Closed-Course Experiment

In this context, we conducted closed course experiments to analyze which direction of the triaxial acceleration sensor mounted on the wheel steering lever is more sensitive to vibrations from road damage. Meanwhile, we use these experiments to verify whether vehicle speed and engine rotational speed per minute (r/min) affect vibration-based road potholes reflectometry. The closed course experiment site with a 3.2 km circular is located at an automotive parts manufacturing plant in Ningbo, Zhejiang, China.

On this closed course, we chose a high-performance Acura TL 3.5L for the field test, which can reach a running speed of 190 km/h in a short time. The following Table I shows the parameter records from the on-board diagnostics port. Although the experimental field is smooth, there are still extremely slight unsmooth areas in the middle part of the field, as shown in Fig. 6. We tried to pass this area at different speeds during the testing period to verify the vehicle speed adaptable to the road roughness identification method. During the experiment, the vibration information presents in Fig. 7.

In Group A, we rapidly speeded up the vehicle to 80 km/h and started vibration observations. In the interval when the road is almost smooth, there is no significant amplitude increase in all three directions of the acceleration sensor. When the vehicle

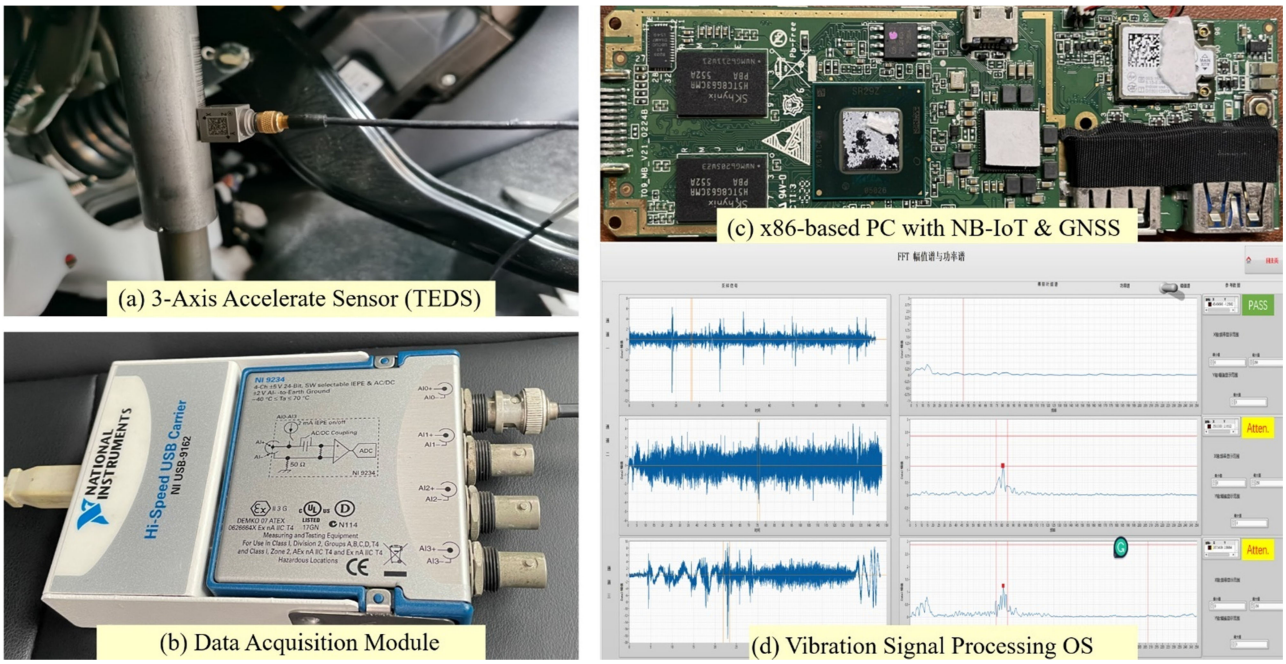

Fig. 4. Principal hardware and software in the prototype cavity. (a) Three-axis acceleration sensor with TEDS. (b), (c) Signal acquisition module and mini-PC module embedded in the cavity. (d) Software system for signal acquisition and automatic processing.

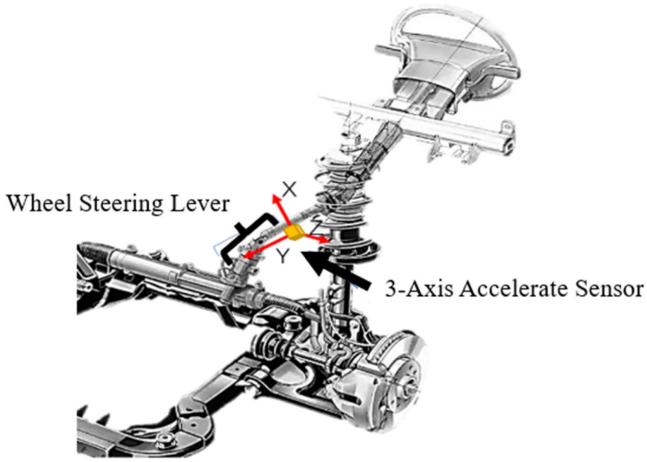

Fig. 5. Installation schematic of the acceleration sensor.

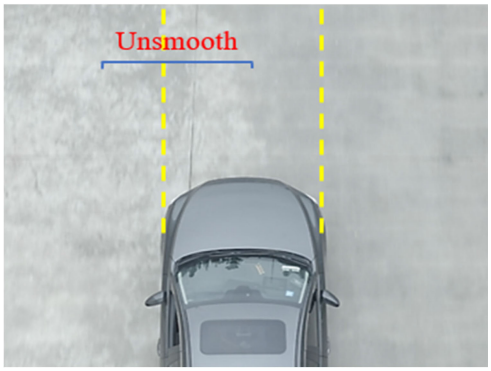

Fig. 6. Slightly rough areas of the road where vehicles pass.

passed over a slight abrasion road surface, the *Y*-axis direction (parallel to the Wheel steering lever), there was a sudden signal change with an amplitude of 0.6 at 60–90 Hz [see Fig. 7(b)]. Still, the *X*-axis [see Fig. 7(a)] and *Z*-axis [see Fig. 7(c)] were almost entirely insensitive to the vibration between 20–100 Hz. In Group B, the cruising speed was increased to 140 km/h and reached 175.2 km/h over the same slight abrasion road surface (GNSS speed measurement). As shown in Fig. 7(e) (parallel to the acceleration direction of the Wheel steering lever), there is still a significant wave around 80 Hz. However, the amplitude of the *X*-axis and *Z*-axis around 80 Hz is not as significant as that of the *Y*-axis.

According to the experimental data, we found that the vibration interface-based road quality fast reflectometry method works normally, and the reflectometry results do not make a significant impact on the speed of the vehicle (i.e., within the speed range of 30–190 km/h). However, when studying these observation data, we found that the level of the sampling frequency of the acquisition card affects the observations of vehicles driving at high speeds, and we will analyze this issue in the discussion. At the same time, it is not difficult to conclude that the acceleration observations direction parallel to the wheel steering lever (Axis Y) is more sensitive to the roughness of the road surface. The horizontal direction of the wheel steering lever (Axis Z) is the second susceptible to the roughness of the ground. Still, the amplitude is already not very significant compared to the Axis Y direction. The road surface roughness hardly affects the direction perpendicular to the wheel steering lever (Axis X). This is due to the fact that when the tire passes over a coarse road surface, the compression and release of the tire in contact with the road surface generates a vertical force relative to the parallel

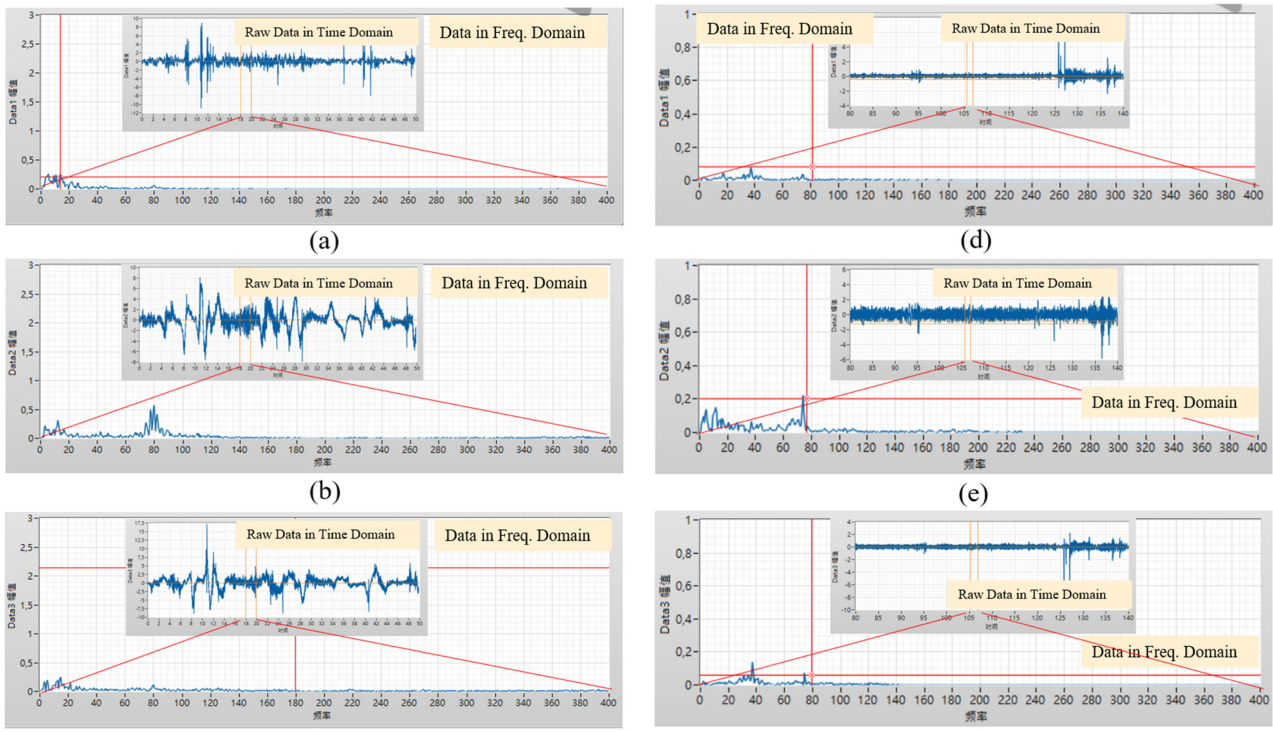

Fig. 7. Effect of different vehicle speeds on the vibration of the steering lever in three directions under the closed course. (a)–(c) Reference to Group A in Table I. (d)–(f) Reference to Group B in Table II. These data are recorded when the vehicle is driven over the area shown in Fig. 6. The velocity does not affect the result of the observations. And its sensitive direction is parallel to the wheel steering lever (vertical to gravity).

direction of the wheel steering lever. And the continuous rolling and release of the tire in contact with the road surface generate a longitudinal force relative to the horizontal direction of the wheel steering lever.

In another aspect, during running and speeding up the vehicle, the r/min of engine speed will enhance with the acceleration. In order to exclude whether the rotation speed of the engine has an effect on the vibration of the steering wheel drive lever, we added an experiment on the effect of engine speed in the parking state. The experiment still uses Acura TL 3.5L for acquiring the vibration signals at idle (neutral position, cutting OFF the transmission input and output). We recorded the vibration signals on the steering wheel drive lever during the experiment at idle (Under 1000 r/min), 2000 r/min, and 3000 r/min. The results are presented in Fig. 8. The vibration signal sampled is in the Axis Y direction.

In the idle state with full throttle release (when the engine speed is lower than 1000 r/min), there is no obvious wave peak around 80 Hz on the spectrum [see Fig. 8(a)], and only a tiny signal exists at 20 Hz, which is the vehicle jitter at idle speed when starting from a cold state. When the throttle is held to 2000 r/min and 3000 r/min, there is still no unmistakable signal around 80 Hz [see Fig. 8(b) and (c)]. The results indicate that the vehicle is driven in a nonintense state (engine speed within 3000 r/min). From the results, it is concluded that the engine speed does not have a significant impact on the vibration of the steering wheel drive lever.

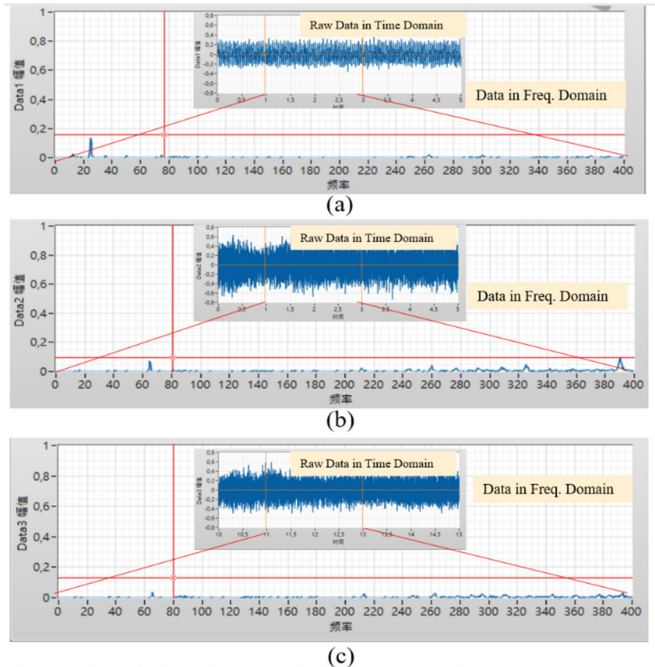

Fig. 8. Effect of engine speed on the observation system. (a) Engine speed below 1000 r/min. (b) Engine speed is maintained at 2000 r/min. (c) Engine speed is maintained at 3000 r/min.

C. Normal Road Condition Experiment

Section III-B presents the results of the vibration tests on the closed course for various vehicle speeds and engine speeds, which only provide a reference for the implementation ability of the method. However, the availability of this method still requires experiments to be completed under normal road conditions. For the actual tests, we selected a portion of the roadway in the Guanggu East area of Wuhan, where the road length is more than 10 km. The condition of the road sections in this area varies and is suitable for road field testing as this area is newly opened. In this context, we performed reproducible experiments based on Acura TL, and Toyota Highlander for a month, up to 10 repetitions on this roadway. This experiment simulates the device's operation installed in the taxis.

First, the context needs to verify this method's effectiveness in municipal road operations. During the experiment, a drone tracked the vehicles and recorded the condition of the road vertically. We selected the DJI Mavic 2 Pro with the Hasselblad camera, which has the ability to track up to 72 km/h and record at 4K 60 FPS. The UAV photography and vibration acquisition equipment operate simultaneously, which helps to compare the data when analyzing the experiment results. This 5 km section of the new municipal road in the Guanggu East area of Wuhan City is generally in serviceable condition, but many places are damaged. Three different levels of damage were selected as typical cases: Slight (accumulated rainwater possible), Obvious (which already affects the driving experience), and Fractured [see Fig. 10(b), (d), and (f)].

Subsequently, the system still needs to determine the reliability of results through the rms calculation to improve the confidence of the observation results. The ratio of the previous second (S-1) to the current time (S) is compared by calculating the rms value of the acquired signal every second in real-time. Fig. 9(a) is a normal road section with $\text{rms}_{(S-1)} = 0.358$ and $\text{rms}_{(S)} = 0.402$, with a ratio of 89%. Fig. 9(b) is in the obviously damaged road section, $\text{rms}_{(S-1)} = 0.481$, $\text{rms}_{(S)} = 1.039$, the ratio is 46%, it can be seen that there is a significant abrupt change in the amplitude of Fig. 9(b). This process can effectively ensure that the results obtained in the frequency domain stage are accurate and enhance the reliability of the system.

Under frequency domain analysis, Fig. 10(a) shows the observed results of the vehicle passing a slight unsmooth road surface, as shown in Fig. 10(b). At 80 Hz in the spectrum [see Fig. 10(a)], the amplitude is less than 1. Due to the excellent NVH performance of modern vehicles, this lightly abrasive road surface is not perceptible to the occupants or the vehicle's driving safety. The spectrum in Fig. 10(c) shows the reflectometry data when the vehicle passes over an obvious rough road surface with an amplitude of 1.2 (About −3.2 dB) at 80 Hz. When the vehicle passes over this road surface [see Fig. 10(d)], the roughness of the road surface is clearly felt by the vehicle occupants. Fig. 10(e) shows the vibration data when the vehicle is driving over the fractured road surface. The amplitude is 1.5 (About −1.4 dB) signal at 80 Hz is evident after the fractured road surface due to the height difference between the two sides of the crack. Such a road surface affects the driving experience and may damage the outer wall of the tire and cause traffic accidents. Fig. 10(g) shows a randomly selected undamaged road surface, where the amplitude at 80 Hz is extremely small for a good quality road surface.

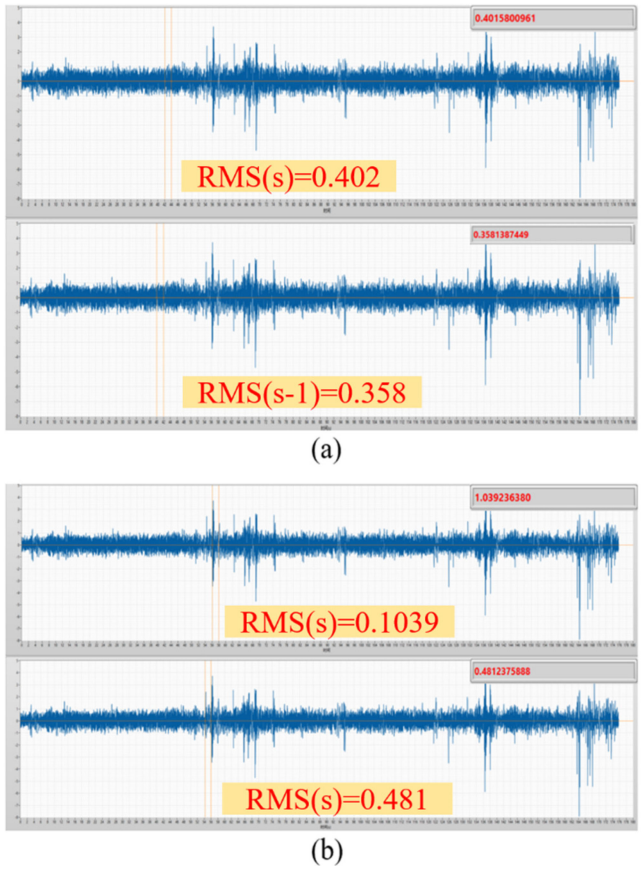

Fig. 9. Comparison of the rms amplitude of the road. (a) Section without damage. (b) Section with obvious damage.

By the experiment on the normal municipal roads, this context proposed that 75–85 Hz is a more sensitive frequency interval for road roughness reflectometry using acceleration sensors mounted on the wheel steering lever. By extracting the frequency amplitude, it is possible to have the reference value for fast road roughness reflectometry. When the road is in a nondamaged state, there is almost no significant signal amplitude around 80 Hz of the spectrum. When the road with the section has different degrees of damage, the signal amplitude around 80 Hz is proportional to the damage. It is expressed that the higher the degree of damage, the greater the signal intensity.

D. Experiments on Prototype Devices

According to the experimental results of Sections III-B and III-C, the acceleration measurement direction parallel to the wheel steering lever is the most sensitive to the reflectometry of road quality. Also, vehicle speed and engine speed do not affect reflectometry results based on the vibration. Also, 80 Hz is a critical parameter for vibration-based reflectometry of road quality, and the degree of damage and the signal amplitude located at 80 Hz are positively correlated. However, these experiments are used to validate the methodology of the prototype and

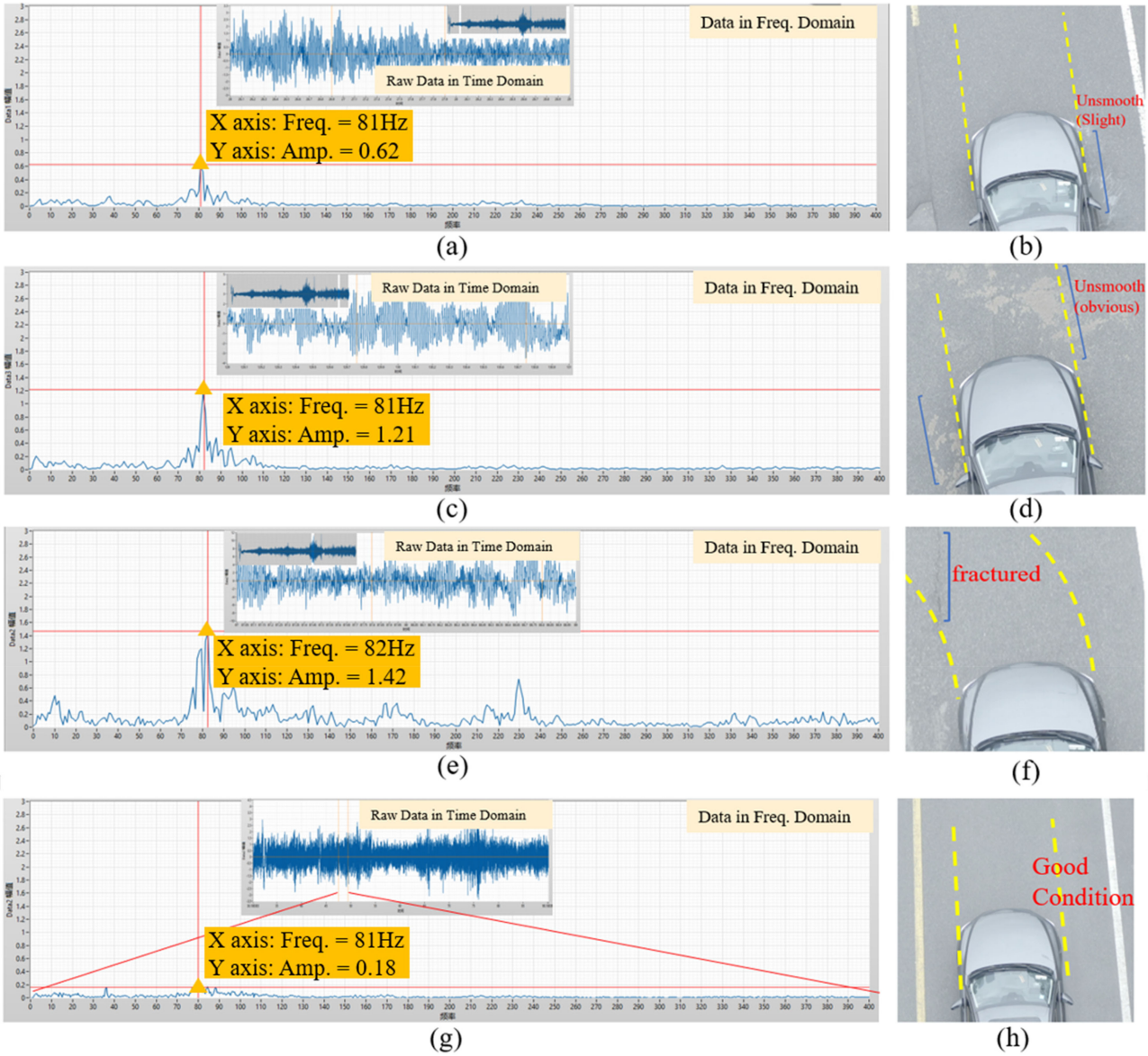

Fig. 10. Results of the normal road conditions experiment. Four conditions are recorded in this figure. (a) Road with slight damage. (c) Road with obvious damage. (e) Fractured road surface. (g) Road surface in good condition. As the vibration sensors begin to acquire signals, the UAV automatically tracks the vehicle and records video of the road vertically for verification, (b), (d), (f), and (h).

the data acquired and analyzed in the developer's mode only. The significance of the method for road quality observations in smart cities still requires experiments with the prototype system.

Fig. 11 presents the results of the automated process in the prototype and the server for real-time GIS service (mapping). In a fully automated acquisition process, the acquisition signal processes with wavelet analysis at a signal frequency between 60 and 90 Hz per second. The signal amplitude will correspond to the system's timestamp, as shown in the Rainbow image in Fig. 11. In this Rainbow image, the system timestamp (horizontal axis), the controlled observation frequency (vertical axis), and the reflection amplitude (color contrast) are included. In wavelet analysis, the amplitude is scaled up by a factor of 100 to improve database management efficiency (as integer data and no longer as float like Sections III-B and III-C). In the database of the prototype system, in addition to the signal data, at the same time, the UTC obtained by GNSS, the latitude and longitude information converted into Plus codes are recorded, as shown in the grid in Fig. 11. Its corresponding database in the prototype device is shown in Table II. It is a part of the data returned from a car installed with road quality reflectometry equipment at 13:05–13:06 on May 7, 2022, located on the Road of Keji second in the East Lake High-tech Zone of Wuhan City. In the database of the prototype system: The edge-side time obtains from the GNSS, and it saves in the TimeStamp as an integer.

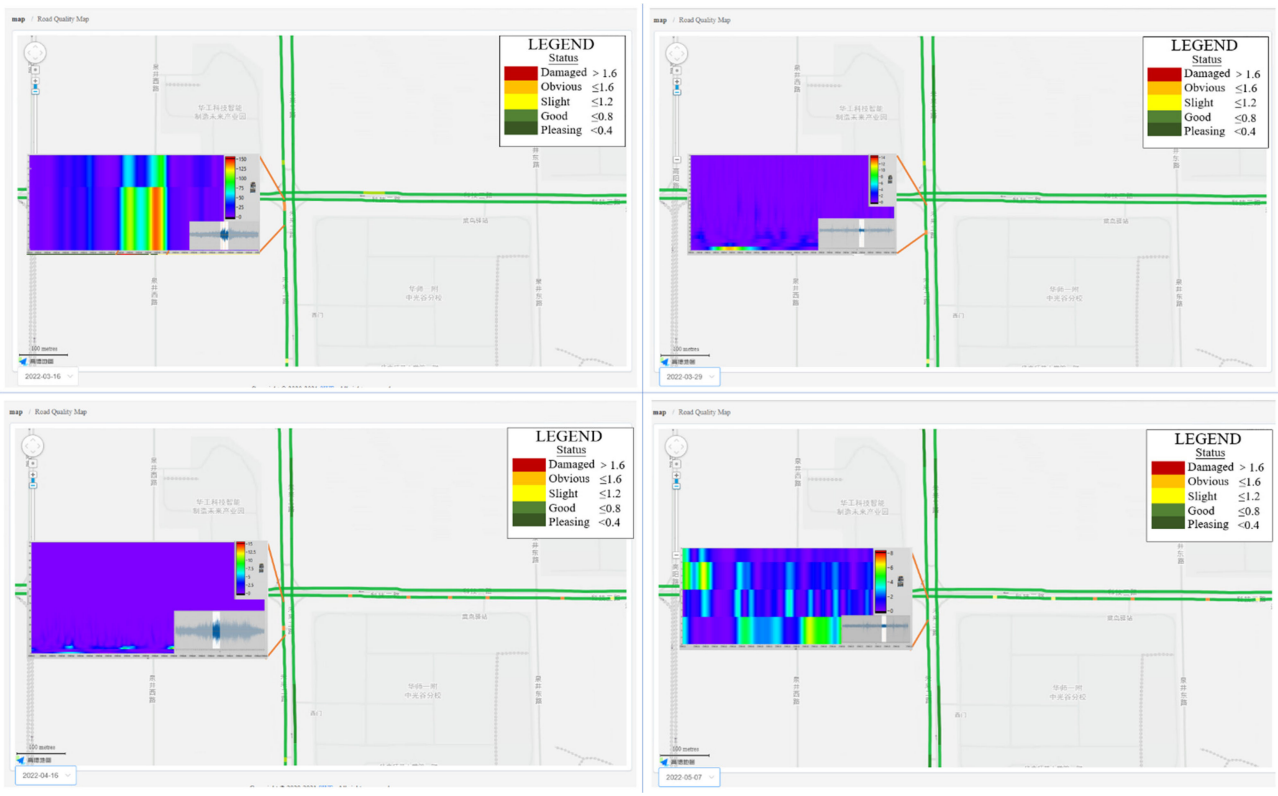

Fig. 11. Web-based map service for road potholes mapping. The road quality reflectometry results (maps services) and raw data (amplitude, time, and frequency determined after wavelet analysis) are selected at different times on the same road section. It can be clearly identified from March to May 2022.

TABLE II
DATABASE EXAMPLE OF THE PROTOTYPE SYSTEM

TimeStamp	GNSS Time (UTC)	Location (Plus Codes)	Vibration Amplitude (*0.01v)
1651899906	20220507130506	8P2PFHHP+QG6	115
1651899909	20220507130509	8P2PFHHP+QMC	140
1651899917	20220507130517	8P2PFHHP+QWG	144
1651899926	20220507130526	8P2PFHHP+QW6	197
1651899939	20220507130539	8P2PFHHQ+QX3	183
1651899947	20220507130547	8P2PFHHR+QR4	117
1651899955	20220507130555	8P2PFHHR+QXH	106
1651899974	20220507130614	8P2PFHHV+Q76	103
1651899989	20220507130629	8P2PFHHV+QJ5	105
1651900002	20220507130642	8P2PFHHV+QX5	107

The longitude and latitude receive from the GNSS data by the edge-side device as Google Plus Code for saving, and the data is of string type. Vibration Amplitude acquires by the acceleration sensor, and it saves as an integer type after being magnified 100 times. Such a database management method helps to improve the efficiency of database processing.

The database on the prototype equipment will be pushed to the server according to IPv4 and Port in JSON format. The data transmit via NB-IoT with a time resolution of 60 s. After the server effectively parses the data, the number of times counted by the abnormal amplitude of the road section (i.e., Plus Codes), which marked on the map in real-time when the threshold value is exceeded.

This demo experiment uses three vehicles with this prototype installed to drive through the road section (i.e., FHGV+8, FHGW+8, and FHGX+8). The road's right lane was under construction and had significant potholes, while the left lane of the road was completed with satisfactory quality. The three vehicles drive over the damaged road surface three times each, and the server generates the data shown in Fig. 11(a). The amplitude of FHGV+8R - FHGV+8X is about 125 $\times$ 0.01v–150 $\times$ 0.01v (damaged). Subsequently, the three vehicles simultaneously drove over the repaired road section. The server updated the data, as shown in Fig. 11(b), the average signal amplitude under 4$\times$0.01v of the road section has been repaired.

IV. DISCUSSION

In Table III, we compared the proposed method with current methods. These methods are more dependent on labor, special vehicles, or loading platforms, while the professional operation and high price bring limitations to the widespread use and deployment of these methods. Although vibration-based monitoring of the quality of roads had also been proposed in the past, there are no environments for independent operation, no edge data processing capability, no precise monitoring spot for the sensors, and a lack of the ability to observe in real-time constructed by the IoT and GIS environment. These problems are solved in this context, and a vibration detection-based road quality reflectometry method is proposed, which combines the

TABLE III
COMPARISON OF DIFFERENT METHODS IN ROAD QUALITY ASSESSMENT

Methodology	Manual observation	Crowdsourcing	Computer Vision	Radar measurements	Vibration Reflectometry
Physical Devices	With Professional instruments: e.g., Roughness measuring instrument;	Smartphones with the camera and Location-Based Services	Monocular or stereo cameras installed on Road Surveillance Network and Intelligent Vehicles	Lidar or Millimeter-wave radar; Synthetic Aperture Radar by UAV or Vehicles	Acceleration sensors; A Mini Size Data Acquisition System and Taxis
Cyber Infrastructure	N/A	With a Software and User app. Data transfer via Internet	Based on a computer system with a GPU and uploads data via a broadband network. Higher power consumption	Based on a computer system with a GPU. Higher power consumption	Low-power system with edge data processing capability, using NB-IoT to transmit observation data and Spatio-temporal information
Observation accuracy	Extremely	Practicable	Referable	Extremely on the road surface; Referable on remote sensing	Referable
Automaticity	Impossible	Impossible	Possible	Impossible	Possible
Real-time capabilities	Impossible	Low	Possible	Impossible	Possible
Aggregate analysis	High cost, complexity, and no real-time support	Limited real-time, and no automatic measurements possible	Requires specialized vehicles, higher computing power and complex deployment	High cost, complexity, and no real-time support	Geo-referenced level observation capability, automated measurements, rapid deployment capability based on spatio-temporal fusion

Web-GIS services to present the real-time reflectometry observation results in the Web-GIS Server. The comparison shows that the road quality reflectometry method based on wheel steering lever vibration observation proposed in this context is bringing reference to the real-time and rapid identification of the quality of roads in future smart cities. With the help of the Web-GIS system of the smart city sensing service platform, it can provide rapid feedback on abnormal road information and improve observation efficiency.

Nevertheless, this article still identified some issues in the experiments that need further investigation. First of all, regarding the sampling rate of the sensor. In Section III-B, we proved the method's effectiveness for the observation in the speed range of 30–190 km/h. However, further research revealed that when passing over the same rough road surface at the same sampling rate, the vibration amplitude located around 80 Hz appears to decrease when the vehicle speed increases. When we try to increase the sampling rate, the observed amplitude of vibration at that frequency will increase accordingly. This issue is brought about by the vehicle passing over a rough road surface at a fast speed. The sampling rate is insufficient, and there may be under sampling, resulting in a decrease in the vibration signal amplitude. Likewise, when the vehicle passes at slow speeds, the sampling rate may be oversampled, resulting in an increase in vibration signal amplitude. Although this problem does not affect the rapid evaluation and inversion of road quality, it impacts the evaluation system of road quality that is on the server-side. For this issue, the team will build an automated control system to control the sampling rate of the acquisition device in real-time with dynamic level control by the change of vehicle speed.

Overall, we believe that the fast reflectometry method of road quality based on vibration observation is valuable in smart cities. This method makes up for the low Spatio-temporal resolution of manual observation and fixed camera observation by continuous Spatio-temporal trajectory and also makes up for the high cost of use and lack of plug-and-play of LiDAR vehicle-mounted computer vision by the vibration monitoring method. This research method has huge application values for road observation in cities. In addition, compared with the legacy method of using electromagnetic waves for earth observation, this context proposes mechanical waves for earth surface observation, which can bring further thoughts for the improvement of earth observation.

Furthermore, with the deployment of the Global Navigation Satellite System and high-density 5G communication base stations on the ground, remote sensing reflection measurements can be performed on the ground through the electromagnetic wave signals transmitted and received by these satellites or base stations, e.g., the Global Navigation Satellite System Reflectometry (GNSS-R) based soil moisture observation [28]. Compared with the soil moisture remote sensing satellites (e.g., Soil Moisture and Ocean Salinity, SMOS, and Soil Moisture Active and Passive, SMAP) [29], the GNSS-R has a higher revisit period and provides near real-time observation data. If the reflection method of the 5G base station near the ground is applied, it can obtain almost real-time and high-precision remote sensing

observation results. This remote sensing technique (electromagnetic wave signals reflectometry) fully applies to road quality or deformation observation [30], but a series of ground correction processes are required. The vibration-based observation strategy provided in this context is valuable to realize the real-time ground correction with the high temporal and spatial resolution for the abovementioned remote sensing ways.

V. Conclusion

High-quality roads condition will enhance the comfort and safety of the driver and passengers. The road surface without the obvious defects improves the speed of the vehicle as much as possible to ensure the efficiency of life and production. However, the temperature, external forces, overloads, and human damage bring road damage. It poses a significant safety risk to vehicles and motorists if the road damage cannot be observed and resolved in time. Although researchers in the past have proposed various methods, they are inadequate in spatial and temporal resolution and efficiency.

In this context, we propose to install acceleration sensors based on the wheel steering lever of the vehicle by capturing the structural vibrations caused by the contact between the vehicle wheels and the road surface. The road roughness is judged by analyzing the amplitude intensity at 60–90 Hz frequency, and real-time analysis and Spatio-temporal information are fused to form a set of rapid reflectometry methods for road quality via the IoT platform. The cumulative analysis of abnormal trajectory information on the server-side provides a set of road defect information maps with a real-time resolution by Web-GIS. It provides a set of reference methods for road management in smart cities and also provides a reference for future vehicle-road cooperation for intelligent driving. In the subsequent research, we will explore the capability of the method to invert other road features at other frequencies. Finally, an attempt has been made to use Google Plus code for geospatial location description in smart city applications in this context. The use of this class of GeoSOT-based (GEOgraphical coordinates Subdividing grid with one-dimension integral coding On 2n-Tree) methods helps to discretize and multiscale the geospatial, and the physical objects can be quickly associated with data within the same area by means of unique integer-type codes for each block, like the Google Plus Code corresponding to the road vibration information under the block in this context. GeoSOT's representation of spatial location is cutting-edge. In the future, in addition to Google Plus Code, Beidou Grid Code will also become more mature, and all observation data obtained based on sensor web and remote sensing methods can be expressed by Beidou Grid Code, which brings excellent development space for the cost, power consumption, and computational pressure of the system of geospatial observation.

References

[1] G. Jianya et al., "Progress and application for intergraded sensing and intelligent decision in smart city," *Acta Geodactica et Cartographica Sinica*, vol. 48, no. 12, pp. 1482–1497, 2019, doi: 10.11947/j.AGCS.2019.20190464.

[2] D. Chen, X. Zhang, and N. Chen, "Smart city awareness base station: A prospective integrated sensing infrastructure for future cities," *Geomatics Inf. Sci. Wuhan Univ.*, vol. 47, no. 2, pp. 159–180, 2022, doi: 10.13203/j.whugis20210224.

[3] S. Chen, W. Ma, B. Wang, S. Xu, and X. Wang, "Research on subjective evaluation method of navigation guidance level-2 automatic driving system," in *Proc. SPIE 12050, Int. Conf. Smart Transp. City Eng.*, Nov. 2021, Art. no. 120505K, doi: 10.1117/12.2613939.

[4] P. Cocron, V. Bachl, L. Früh, I. Koch, and J. F. Krems, "Hazard detection in noise-related incidents – the role of driving experience with battery electric vehicles," *Accident Anal. Prevention*, vol. 73, pp. 380–391, 2014.

[5] S. Nath, J. Liu, and F. Zhao, "SensorMap for wide-area sensor webs," *Computer*, vol. 40, no. 7, pp. 90–934, Jul. 2007.

[6] C. Gaffney and C. Robertson, "Smarter than smart: Rio de janeiro's flawed emergence as a smart city," *J. Urban Technol.*, vol. 25, no. 3, pp. 47–64, 2018.

[7] N. Chen, X. Yang, and X. Wang, "Design and implementation of geospatial sensorweb information public service platform," *J. Geo-Inform. Sci.*, vol. 15, no. 6, pp. 887–894, 2013.

[8] I. Shahrour and X. Xie, "Role of internet of things (IoT) and crowdsourcing in smart city projects," *Smart Cities*, vol. 4, no. 4, pp. 1276–1292, Oct. 2021, doi: 10.3390/smartcities4040068.

[9] W. Li, M. Burrow, and Z. Li, "Automatic road condition assessment by using point laser sensor," in *Proc. IEEE Sensors*, 2018, pp. 1–4, doi: 10.1109/ICSENS.2018.8589855.

[10] M. Cheng, H. Zhang, C. Wang, and J. Li, "Extraction and classification of road markings using mobile laser scanning point clouds," *IEEE J. Sel. Topics Appl. Earth Observ. Remote Sens.*, vol. 10, no. 3, pp. 1182–1196, Mar. 2017.

[11] H. Guan, J. Li, Y. Yu, M. Chapman, and C. Wang, "Automated road information extraction from mobile laser scanning data," *IEEE Trans. Intell. Transp. Syst.*, vol. 16, no. 1, pp. 194–205, Feb. 2015.

[12] Y. Li, C. Papachristou, and D. Weyer, "Road pothole detection system based on stereo vision," in *Proc. IEEE Nat. Aerosp. Electron. Conf.*, 2018, pp. 292–297, doi: 10.1109/NAECON.2018.8556809.

[13] A. Dhiman and R. Klette, "Pothole detection using computer vision and learning," *IEEE Trans. Intell. Transp. Syst.*, vol. 21, no. 8, pp. 3536–3550, Aug. 2020, doi: 10.1109/TITS.2019.2931297.

[14] R. Fan, U. Ozgunalp, B. Hosking, M. Liu, and I. Pitas, "Pothole detection based on disparity transformation and road surface modeling," *IEEE Trans. Image Process.*, vol. 29, pp. 897–908, 2020, doi: 10.1109/TIP.2019.2933750.

[15] A. Babu, S. V. Baumgartner, and G. Krieger, "Approaches for road surface roughness estimation using airborne polarimetric SAR," *IEEE J. Sel. Topics Appl. Earth Observ. Remote Sens.*, vol. 15, pp. 3444–3462, 2022, doi: 10.1109/JSTARS.2022.3170073.

[16] L. Krysiński and J. Sudyka, "GPR abilities in investigation of the pavement transversal cracks," *J. Appl. Geophys.*, vol. 97, pp. 27–36, Oct. 2013.

[17] P. M. Harikrishnan and V. P. Gopi, "Vehicle vibration signal processing for road surface monitoring," *IEEE Sensors J.*, vol. 17, no. 16, pp. 5192–5197, Aug. 2017, doi: 10.1109/JSEN.2017.2719865.

[18] C. J. Dodds and J. D. Robson, "The description of road surface roughness," *J. Sound Vib.*, vol. 31, no. 2, pp. 175–183, 1973.

[19] C. Wu et al., "An automated machine-learning approach for road pothole detection using smartphone sensor data," *Sensors*, vol. 20, no. 19, Sep. 2020, Art. no. 5564, doi: 10.3390/s20195564.

[20] T. Wu, H. Shen, J. Qin, and L. Xiang, "Extracting stops from spatio-temporal trajectories within dynamic contextual features," *Sustainability*, vol. 13, no. 2, Jan. 2021, Art. no. 690, doi: 10.3390/su13020690.

[21] P. Kindt, F. De Coninck, P. Sas, and W. Desmet, "Analysis of tire/road noise caused by road impact excitations," *SAE Technical Paper 2007-01-2248*, 2007, doi: 10.4271/2007-01-2248.

[22] C. Zhao, Y. Xing, and H. Wang, "Method to improve vehicle noise excitated with some road," *Auto Electric Parts*, vol. 7, pp. 30–33, 2018, doi: 10.13273/j.cnki.qcdq.2018.07.016.

[23] H. E. B. Russell and J. C. Gerdes, "Design of variable vehicle handling characteristics using four-wheel Steer-by-Wire," *IEEE Trans. Control Syst. Technol.*, vol. 24, no. 5, pp. 1529–1540, Sep. 2016, doi: 10.1109/TCST.2015.2498134.

[24] S. McRobbie, A. Wright, J. Iaquinta, P. Scott, C. Christie, and D. James, "Developing new methods for the automatic measurement of raveling a traffic-speed," in *Proc. 11th Int. Conf. Asphalt Pavements*, 2010, pp. 1–10.

[25] W. Shi, M. Li, J. Guo, and K. Zhai, "Evaluation of road service performance based on human perception of vibration while driving vehicle," *J. Adv. Transp.*, 2020, Art. no. 8825355, doi: 10.1155/2020/8825355.

[26] D. Chen, C. Cheng, S. Song, F. Dong, and R. Chen, "Research of spatial topological relation model based on GeoSOT," in *Proc. IEEE Int. Geosci. Remote Sens. Symp.*, 2013, pp. 786–789, doi: 10.1109/IGARSS.2013.6721275.

[27] C. Qian, C. Yi, C. Cheng, G. Pu, X. Wei, and H. Zhang, "GeoSOT-Based spatiotemporal index of massive trajectory data," *ISPRS Int. J. Geo-Inf.*, vol. 8, no. 6, Jun. 2019, Art. no. 284, doi: 10.3390/ijgi8060284.

[28] W. Du et al., "Online soil moisture retrieval and sharing using geospatial web-enabled BDS-R service," *Comput. Electron. Agriculture*, vol. 121, pp. 354–367, 2016, doi: 10.1016/j.compag.2016.01.005.

[29] H. Ma, J. Zeng, N. Chen, X. Zhang, M. H. Cosh, and W. Wang, "Satellite surface soil moisture from SMAP, SMOS, AMSR2 and ESA CCI: A comprehensive assessment using global ground-based observations," *Remote Sens. Environ.*, vol. 231, 2019, Art. no. 111215.

[30] Y. Chen, S. Yan, and J. Gong, "Phase error analysis and compensation of GEO-satellite-based GNSS-R deformation retrieval," *IEEE Geosci. Remote Sens. Lett.*, vol. 19, 2022, Art. no. 2506505, doi: 10.1109/LGRS.2022.3187561.

Dong Chen (Member, IEEE), received the B.S. degree in electronic and automatic from University of Lorraine, Metz, France, in 2016 and the M.S. degree in human-machine automation system engineering from Laboratory of Systems Design, Optimization, and Modeling, University de Lorraine, Metz, France, in 2018. He is currently working toward the Ph.D. degree in geospatial information system engineering with State Key Laboratory of Information Engineering in Surveying, Mapping, and Remote Sensing, Wuhan University, Wuhan, China.

He is currently engaged in the research of Internet of Things and Smart Cities during pursuing the Ph.D. degree in Wuhan University. His research interests focus on the high-precision intelligent Geospatial Sensor Web with a fusion of in situ sensor web based on Internet of Things and the UAV/satellite remote sensing. His research interests include the signal processing and identification, biological sensors network, and automatic controlling system.

Nengcheng Chen received the B.Sc. degree in geodesy from the Wuhan Technical University of Surveying and Mapping, Wuhan, China, in 1997, and the M.S. degree in geographical information system and the Ph.D. degree in photogrammetry and remote sensing from Wuhan University, Wuhan, China, in 2000 and 2003, respectively.

From 2006 to 2008, he was a Postdoctoral Research Associate with the Center for Spatial Information Science and Systems, George Mason University, Fairfax, VA, USA. From 2008 to 2021, he was a Full Professor with the State Key Laboratory of Information Engineering in Surveying, Mapping and Remote Sensing, Wuhan University, where he led the Smart Earth Team. From 2021, he was invited to be the Director with the National Engineering Research Center of Geographic Information System (GIS), also the Full Professor with the China University of Geosciences, Wuhan, China. He has authored and coauthored three books and more than 200 research papers. He was also leading author of the technical report of integrated management for smart sustainable city in ITU-T FG-SSC. His current research interests include sensor web, big data, real-time GIS, and smart city.

Xiang Zhang received the Ph.D. degree in cartography and geography information system from Wuhan University, Wuhan, China, in 2017.

From 2017 to 2021, he was an Associate Researcher with Wuhan University. He is currently a Full Professor with China University of Geosciences, Wuhan, China. In recent years, he has received several grants (more than 3.7 million RMB), authorized 3 patents, and authored and coauthored more than 60 SCI/EI/CSCD papers in ESR, RSE, WRR, and IEEE TGRS. Moreover, he was rewarded as "Outstanding Contribution in Reviewing for RSE. His research interests include Spatio-temporal data fusion, drought disaster, and smart sustainable city.

Yuhang Guan received the B.Sc. degree in Internet of Things engineering from Hubei University of Technology, Wuhan, China, in 2019. He is currently working toward the master's degree in the research of Electronic Information with China University of Geosciences, Wuhan, China.

His research interests include smart city, sensor web, and information technology.